Journal of ELECTRONIC MATERIALS, Vol. 38, No. 1, 2009
DOI: 10.1007/s11664-008-0541-1

Interfacial Reaction and Wetting Behavior Between Pt and Molten Solder

S.C. YANG,[1] W.C. CHANG,[1] Y.W. WANG,[1] and C.R. KAO[1,2]

1.—Department of Materials Science & Engineering, National Taiwan University, Taipei City, Taiwan. 2.—e-mail: crkao@ntu.edu.tw

Platinum does not oxidize easily, and has slow reaction rates with Sn-based solders. Due to these two positive attributes, a single platinum layer has the potential to replace both the oxidation protection layer and the diffusion barrier layer in the underbump metallurgy of flip-chip devices. To evaluate this potential further, the dissolution rate and the wetting properties of Pt were investigated in this study. It was found that Pt did have a dissolution rate less than half that of Ni, currently the most popular barrier layer material. The wetting properties of Pt were not as good as those of Ni but were nevertheless still acceptable for industrial applications. In short, as far as the dissolution and the wetting characteristics are concerned, Pt is an effective top surface layer for use in underbump metallurgy.

Key words: Platinum, intermetallic, diffusion, nickel, dissolution

INTRODUCTION

In microelectronic, optoelectronic, and microelectromechanical systems (MEMS) packages, the contact pads for soldering have a multiple-layer structure, including typically an oxidation protection layer, a diffusion barrier layer, and a wetting layer. A good example of this multiple-layer structure is the Au/Ni/Cu trilayer structure, where the Au layer is included for oxidation protection, Ni for diffusion barrier function, and Cu for wetting. The necessity to deposit multiple metal layers to form contact pads adds not only production cost but also design complexity, which always leads to higher reliability concerns. Accordingly, there is a strong driving force to simplify the multiple-layer structure.

The element Pt does not oxidize easily, and has slow reaction rates with Pb-Sn solders,[1–5] Sn-Cu and Sn-Ag-Cu solders,[6] and pure Sn.[7] Because of these two positive attributes, a single platinum layer can serve dual functions as both the oxidation protection layer and the diffusion barrier layer. In fact, several feasibility studies of using a Pt layer in flip-chip solder joints have been reported,[3–5] and the consensus was that Pt exhibited several promising characteristics worthy of further evaluation.

Two types of fundamental data are required before the use of a Pt layer for contact pads can be fully evaluated. The first is the dissolution kinetics of Pt into molten solders. During the assembly of devices, the solder joints have to experience several reflows, during which Pt is in direct contact with the molten solder. The dissolution kinetic data are required in order to determine the proper Pt thickness to be used. The second fundamental data required are the wetting characteristics of molten solders on Pt. In order to have reliable solder joints, solders have to wet the Pt surface in a reasonable amount of time during assembly. The objectives of this study are to establish these two types of data. The dissolution kinetic data were obtained by reacting Pt with pure Sn at 250°C, 270°C, 290°C, and 310°C for different periods of time. For comparison, the dissolution kinetic data of Ni and Co were also measured. The wetting characteristics of Pt with the Pb-Sn eutectic solder at 230°C were studied by using the wetting balance method. The wetting characteristics of Ni

(Received February 29, 2008; accepted August 6, 2008; published online September 10, 2008)

were measured under the same conditions for comparison.

EXPERIMENTAL

Dissolution Kinetics Measurement

Sn solder baths were prepared from 99.99% purity elemental Sn. Each solder bath was formed by placing 6 g Sn into a 10-mm-inner-diameter vial. Nickel disks (6.35 mm in diameter, 99.99% pure), cobalt disks (6.35 mm in diameter, 99.99% pure), and Pt foils (5 mm × 10 mm × 0.1 mm thick) were used to react with the Sn baths. Before the reaction, each metal disk or foil was metallurgically polished on both surfaces. One micrometer of diamond abrasive was used as the last polishing step. The original thickness of each disk or foil was then measured by using a micrometer screw gauge with 1 μm accuracy. At least ten measurements were made on different regions of each disk or foil, and the average value was recorded. These disks and foils were then cleaned with acetone, etched in a 50 vol.% HCl-H_2O solution for 30 s, and fluxed with a mildly activated rosin flux. Each disk or foil was then inserted into a fresh molten Sn bath. The reaction temperatures used were 250°C, 270°C, 290°C, and 310°C, and the reaction time ranged from 1 h to 25 h. When each reaction time was reached, the solder bath together with the metal disk or foil was cooled to room temperature by using an air-blower. The liquid Sn solidified with little disturbance, and cooled to touch in about 90 s. The solidified Sn along with the disk or foil was then removed from the vials, mounted in epoxy, sectioned by using a low-speed diamond saw, and metallurgically polished in preparation for characterization.

The reaction zone for each sample was examined using an optical microscope and a scanning electron microscope (SEM). The compositions of the reaction products were determined using an electron microprobe (EPMA), operated at 15 keV. In microprobe analysis, the concentration of each element was measured independently, and the total weight percentage of all elements was within 100 ± 1% in each case. For every data point, at least four measurements were made and the average value is reported. The remaining thickness of the metal disk or foil after the reaction was measured at regular intervals on its SEM or optical microscope image. For each sample, about 30 data points were measured, and the average thickness was recorded. The consumed thickness was determined by comparing the original thickness and the remaining thickness of each sample.

Wetting Balance Test

The wetting tests were performed by using a Rhesca SAT-5000 (Tokyo, Japan) wetting balance. The Ni and Pt test coupons with 0.1 mm × 2 mm × 15 mm dimensions were cut from 99.99% Ni and Pt foils, respectively. The test coupons were polished, degreased in a 50 vol.% HCl-H_2O solution for 30 s, and then fluxed. The solder baths were prepared from commercial eutectic Pb-Sn solder. Fresh solder bath was used for each test coupon, and the solder baths were kept at 230°C. Two different kinds of fluxes, a water-soluble type and a rosin mildly activated (RMA) type, were used. The immersion speed, immersion depth, and immersion time were 10 mm/s, 4 mm, and 10 s, respectively.

RESULTS

Microstructures of the Reaction Products

After the reaction, the main reaction product between Pt and Sn was $PtSn_4$, as shown in Fig. 1a. At all the other times and temperatures used in this study, $PtSn_4$ was always the main reaction product. These $PtSn_4$ grains had a morphology of orthorhombic plates, as shown in Fig. 1b. X-ray diffraction pattern (Fig. 2) revealed that $PtSn_4$ had the $PdSn_4$ prototype crystal structure. However, when the reaction time increased to 25 h at 250°C, two additional very thin layers of compounds were visible between $PtSn_4$ and Pt, as shown in Fig. 3a. From the EPMA line scan shown in Fig. 3b, these thin layers seemed to be Pt_2Sn_3 and Pt_3Sn. Nevertheless, more studies are required to positively identify these two compounds. These two phases also appeared in the reactions at 270°C, 290°C, and 310°C.

The evolution of the microstructure during the dissolution at 270°C is shown in Fig. 4. The dissolution at the other temperatures showed a similar trend. The thickness of Pt decreased gradually as the amount of $PtSn_4$ increased. These $PtSn_4$ grains formed a dense layer near the interface, but away from the interface became a loose aggregate of orthorhombic plates, radiating away from the interface. The amount of $PtSn_4$ near the interface should not be used to estimate how much Pt had been consumed because the amount of $PtSn_4$ near the interface did not adequately describe the total amount of $PtSn_4$ formed. The overall distribution of $PtSn_4$ is presented in Fig. 5, which shows a vertical cross-section of the entire Pt foil. As can be seen, the distribution of $PtSn_4$ along the depth of the Sn bath was not homogeneous, with more $PtSn_4$ near the top side of the Pt foil and a large amount of $PtSn_4$ near the bottom side of the Sn bath. This distribution pattern was clearly caused by convection in the molten Sn bath. According to our observations, this convection effect became more obvious for temperatures of 290°C to 310°C and for reaction times ranging from 16 h to 25 h. The temperatures of the Sn baths were well controlled within ±1°C, but apparently this small temperature variation combined with the concentration gradient was able to induce a density gradient, which in turn was able to cause enough liquid convection to generate the $PtSn_4$ distribution pattern shown in Fig. 5.

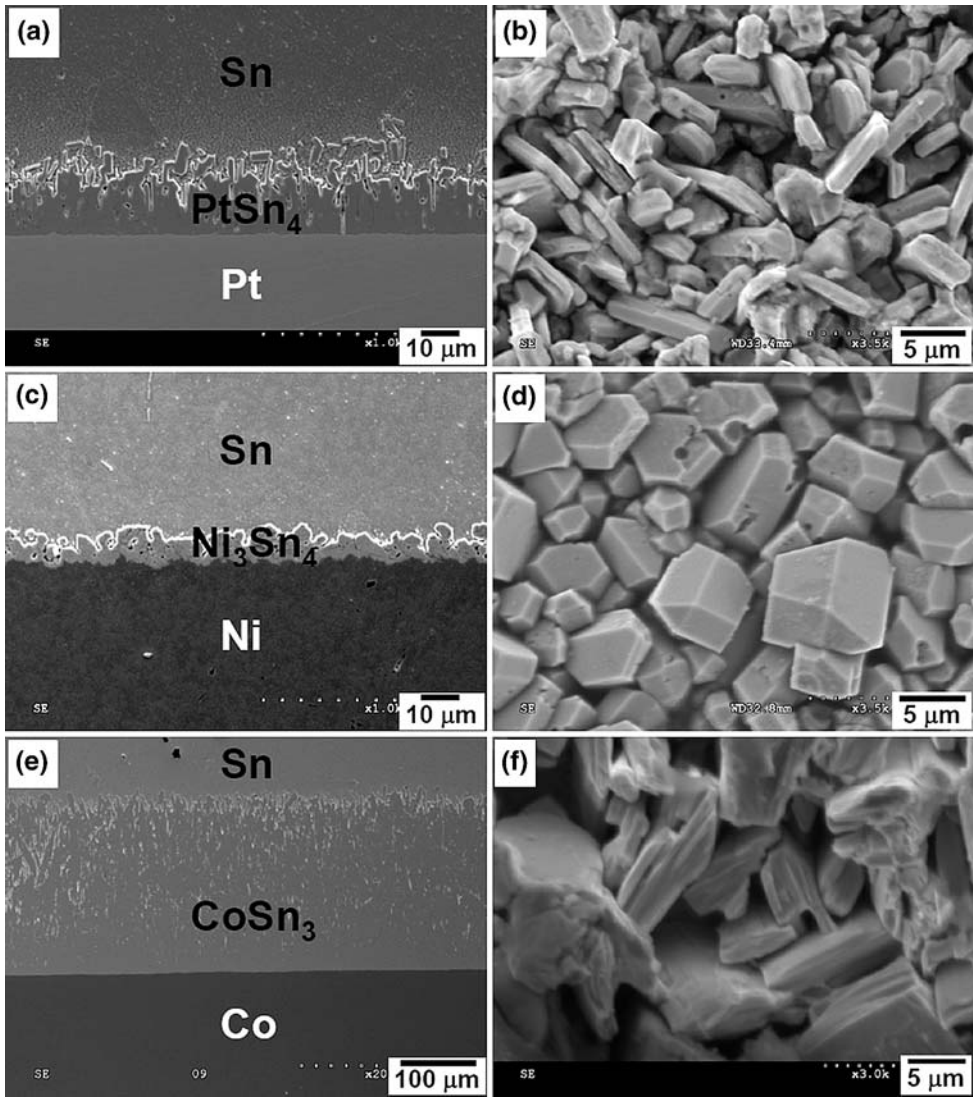

Fig. 1. (a) Interface for the reaction between Sn and Pt at 250°C for 9 h. The main reaction product was $PtSn_4$. This picture is a cross-sectional view with the sectioning plane perpendicular to the Pt surface. At all the other times and temperatures, $PtSn_4$ was always the main reaction product. (b) Top view showing the grain structure of $PtSn_4$. The solder had been etched away with acids. (c and d) Same as (a) and (b), but with Ni as the substrate and Ni_3Sn_4 as the main reaction product. (e and f) Same as (a) and (b), but with Co as the substrate and $CoSn_3$ as the main reaction product.

For comparison, the interface for the Ni-Sn system after the reaction is shown in Fig. 1c and d, and that for the Co-Sn system in Fig. 1e and f. As can be seen in Fig. 1c, the only compound formed at the interface was Ni_3Sn_4 when Ni reacted with Sn. At all other temperatures and times used in this study, only Ni_3Sn_4 formed, which is consistent with the literature results.[8–12] These Ni_3Sn_4 grains had an aspect ratio close to 1, as shown in Fig. 1d. The thickness of Ni_3Sn_4 was only about one-third of the thickness of $PtSn_4$ at the same reaction conditions. The reaction between Co and Sn only produced $CoSn_3$, as shown in Fig. 1e. At all the other temperatures and times used in this study, only $CoSn_3$ formed. This observation was consistent with the study reported in the literature.[13] Under the same experimental conditions, the Co-Sn reaction produced the thickest reaction product among the three binary systems in this study, about twice that of the Pt-Sn reaction. As shown in Fig. 1f, these $CoSn_3$ grains also had a rod-type morphology, with an aspect ratio near that of $PtSn_4$. One key difference between $PtSn_4$ and $CoSn_3$ was that the former formed a compact and protective layer, whereas the latter formed a nonprotective, loose aggregate structure.

Growth Kinetics

Figure 6 shows a comparison of the consumed thickness of Pt, Ni, and Co at 250°C. Platinum had the slowest dissolution rate, and Co the highest. Figure 7 shows that this trend is also true at all the

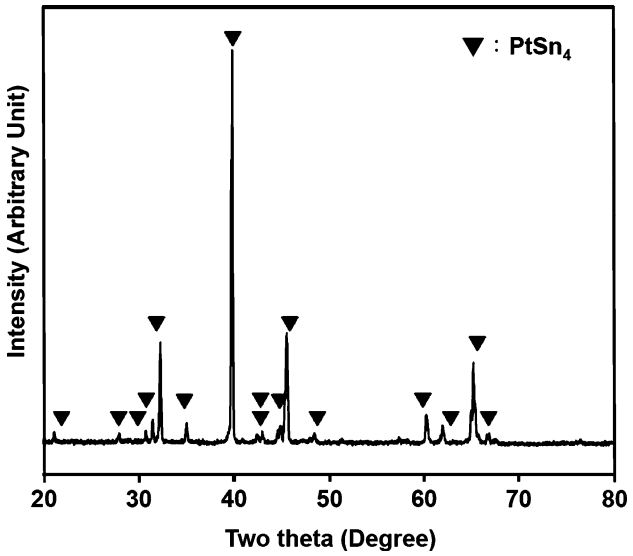

Fig. 2. X-ray diffraction pattern of the reaction product from the Pt-Sn reaction at 250°C for 16 h, showing the formation of the oC20 $PtSn_4$ phase (prototype $PdSn_4$).

other temperatures used in this study. The above results suggest that at all temperatures the Pt layer in underbump metallurgy (UBM) or surface finishes can outlast a Ni layer with the same thickness. In short, Pt will perform much better than Ni or Co as far as the consumption rate is concerned when used as a diffusion barrier layer in UBM or surface finishes.

The dissolution kinetics for Pt in Sn is summarized in Fig. 8. The data were better described by linear kinetics than by parabolic kinetics. Accordingly, the thickness versus time data were fitted to the equation, $d = kt$, where d is the consumed thickness of Pt in meters and t is the reaction time in seconds, to obtain the growth constant k in meters per second. The activation energy for k was then obtained by plotting ln k versus the inversed temperature, as shown in Fig. 9. From the slope of the line in Fig. 9, the activation energy was determined to be 16 kJ/mol.

Wetting Balance Test

Figure 10 shows the wetting curve for the Pt foil in the Pb-Sn eutectic solder at 230°C using the water-soluble-type flux. The force reading of the balance was customarily set to zero when the coupon was freely held before the experiment started. Four kinds of information, the wetting time (t_0), the wetting force (F_m), the withdrawing force (F_w), and the residual force (F_d), can be determined from the wetting curve. However, the wetting time and wetting force are the key indicators for evaluating wettability. The wetting time is defined as the time required for the wetting curve to return to the zero force point, and is 1.46 s for the curve in Fig. 10. Shorter wetting time indicates faster spreading of

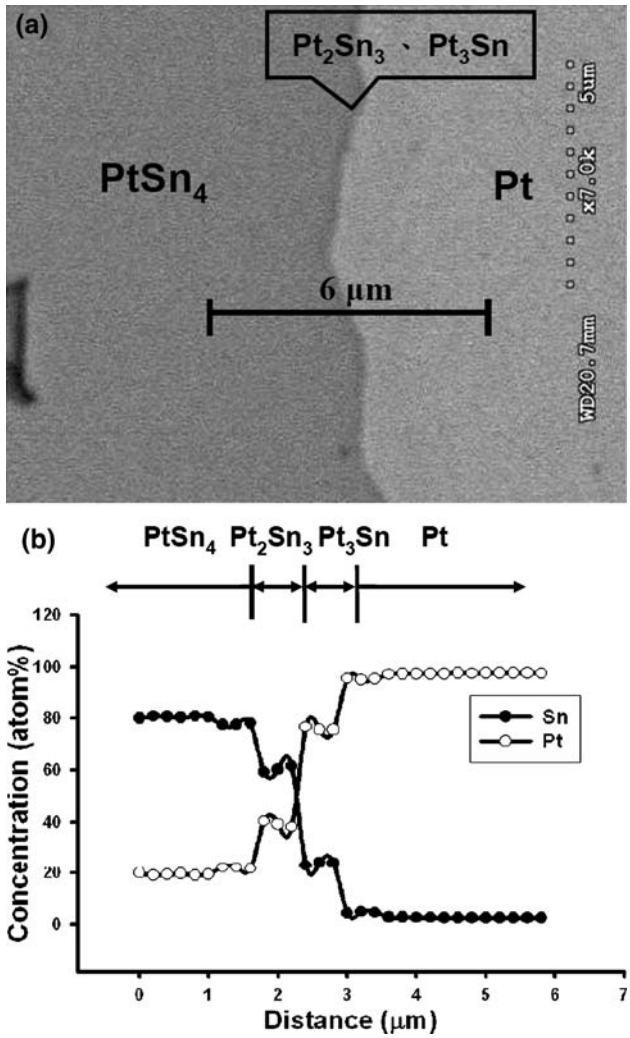

Fig. 3. (a) Zoom of the interface for the reaction between Sn and Pt at 250°C for 25 h. Two additional thin layers of compounds existed between $PtSn_4$ and Pt. (b) EPMA line scan across the interface in (a). According to their compositions, these thin layers seemed to be Pt_2Sn_3 and Pt_3Sn.

the solder on the substrate, and represents good wetting. The wetting force is the maximum force of the plateau region and is 0.9 mN for the curve in Fig. 10. Larger wetting force also indicates better wetting.

Figure 11a presents the average wetting time for the Pt and Ni substrates with the RMA-type and water-soluble fluxes at 230°C. Since shorter wetting time indicates better wetting, it was concluded that the Ni substrate exhibited better wetting than did Pt. Although the wetting time of the Pt substrate was not as good, it still neared the acceptable range. Industry typically would like to have a wetting time less than 1 s. It should be noted that the two types of flux used in this study were commercial ones, and were optimized for use with Ni or Cu substrates. Once new fluxes, optimized for use with Pt, are available, the wetting time for Pt might be reduced further. Figure 11b shows the average wetting force

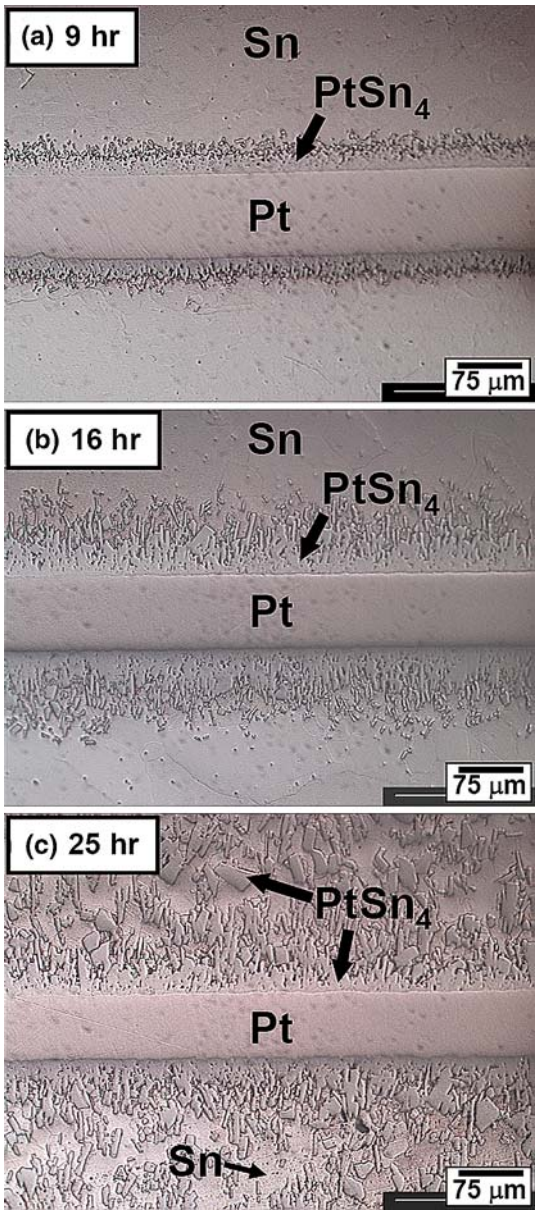

Fig. 4. Evolution of the microstructure during the dissolution of Pt in Sn at 270°C.

Fig. 5. Vertical cross-sectional view of the entire Pt foil after reaction at 310°C for 16 h. This cross-section was cut along the length (10 mm side) of the Pt foil. The top of the micrograph was near the top surface of the Sn bath, and the bottom was near the bottom of the Sn bath.

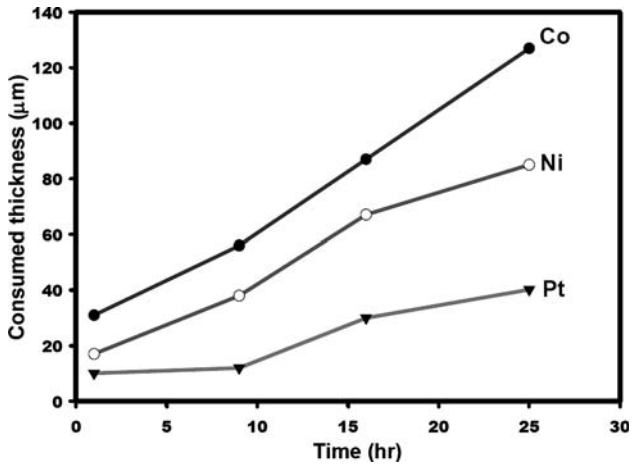

Fig. 6. Consumed Pt, Ni, and Co thickness versus dissolution time at 250°C.

for the Pt and Ni substrates with the RMA-type and water-soluble fluxes at 230°C. The results indicate that Ni performed slightly better than Pt, but for practical purposes they were both more than acceptable for industrial applications. For both the wetting time and wetting force indicators, the water-soluble flux was more effective than the RMA-type flux because the former has more acid component.

DISCUSSION

Figure 1 shows that the intermetallic at the interface for the Pt substrate was much thicker than that for the Ni substrate, even though the consumed Pt thickness was only half that of Ni (Fig. 6). The reason for this apparent discrepancy was that one mole of Pt atoms was able to react with four moles of Sn to form one mole of $PtSn_4$, while one mole of Ni atoms could only react with 4/3 moles

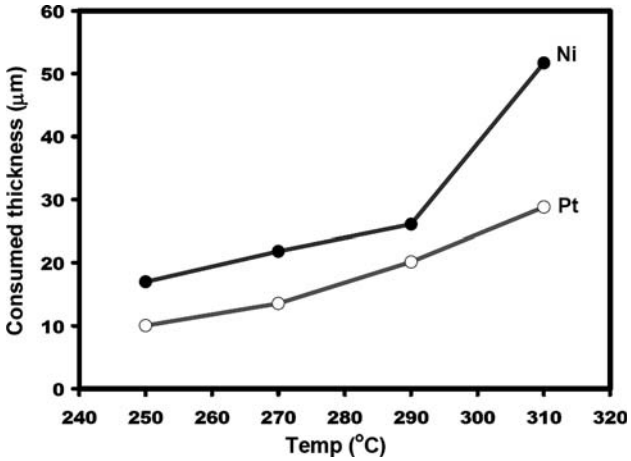

Fig. 7. Consumed Pt and Ni thickness at different temperatures after 1 h of dissolution.

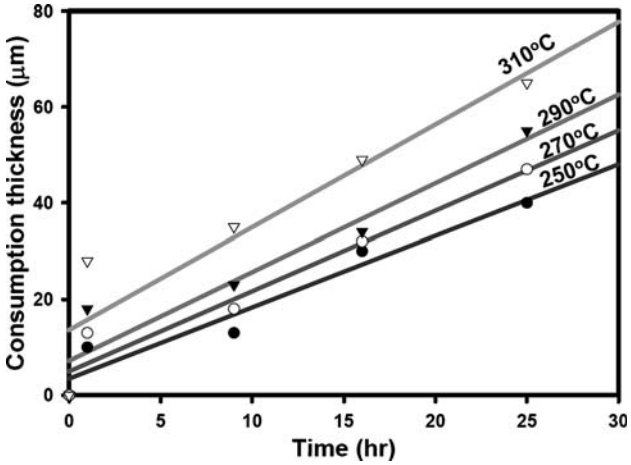

Fig. 8. Consumed Pt thickness versus the dissolution time at 250°C to 310°C.

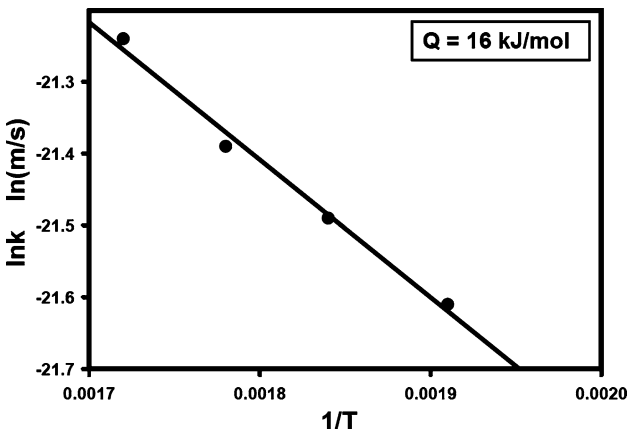

Fig. 9. Arrhenius plot of the Pt dissolution rate constant *k*. From the slope, the activation energy was determined to be 16 kJ/mol.

of Sn to form 1/3 mole of Ni_3Sn_4. In short, a small amount of Pt was able to react with a large amount of Sn to form a thick layer of $PtSn_4$.

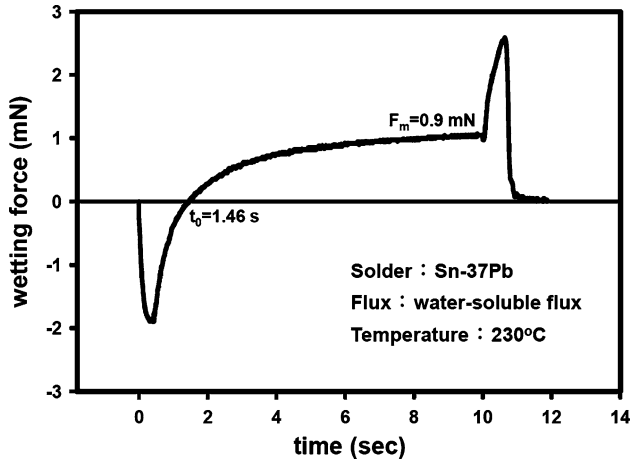

Fig. 10. Typical wetting curve for the Pb-Sn eutectic solder on Pt substrate at 230°C.

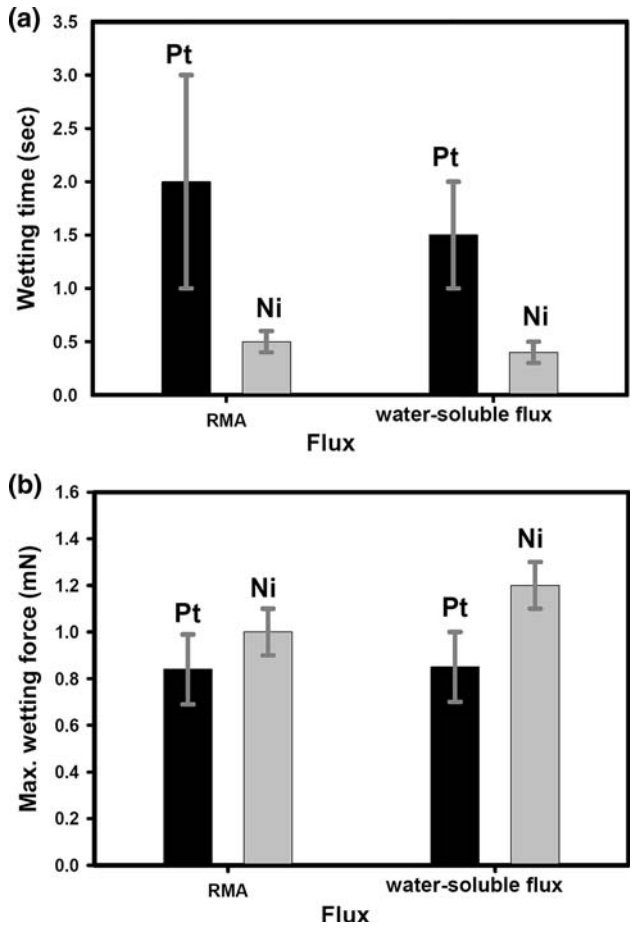

Fig. 11. Comparison of (a) wetting time and (b) wetting forces on Pt and Ni substrates at 230°C.

Platinum is quite unique among noble metals in that it exhibits a very low dissolution rate with molten solders. Many of the noble metals, such as Au,[1,14–20] Pd,[1,5,21] or Ag,[1] react very quickly with solders. This is due to the fact that the intermetallic compound formed at the interface for Pt is more

protective, as illustrated in Fig. 1a. The reaction products from the reactions between Au, Pd, and Ag and the solder were less compact, and as a result less protective. Therefore, their dissolution rates are much higher. The reaction product from the reaction between Co and the solder was also not protective, as shown in Fig. 1e. Accordingly, Co exhibited a faster dissolution rate than Pt, as shown in Fig. 6.

According to the Pt-Sn phase diagram,[22] there are five stable compounds at the temperatures used in this study: Pt_3Sn, PtSn, Pt_2Sn_3, $PtSn_2$, and $PtSn_4$. In this study, the main reaction product was $PtSn_4$, which was always present in a large amount in all samples. When the reaction time increased, two other compounds, probably Pt_2Sn_3 and Pt_3Sn based on the EPMA evidence, were detected. In all the previous studies,[1–7] only $PtSn_4$ was observed. This present study shows that, given time, the other stable compounds on the phase diagram might form.

The saturation limits of Pt in molten Sn at different temperatures can be read directly from the Pt-Sn binary phase diagram,[22] and are 1 wt.%, 1.2 wt.%, 1.4 wt.%, and 2.0 wt.% at 250°C, 270°C, 290°C, and 310°C, respectively. As the Pt substrates were consumed, the Pt concentration in the molten solder increased. From the dimension of the Pt substrate and the mass of the solder bath used, the thickness of the Pt substrate that had to be dissolved in order to make the solder baths become saturated with Pt can be calculated to be 12 μm, 15 μm, 17 μm, and 25 μm at 250°C, 270°C, 290°C, and 310°C, respectively. According to Fig. 8, this amount of Pt could be dissolved in about 1 h at each temperature. In other words, before 1 h, the solder baths were not saturated with Pt, and after 1 h the baths were saturated with Pt. The kinetics reported in this study mainly belongs to the region that the solder had already been saturated with Pt. To study the dissolution kinetics for the region far from saturation, different experimental designs have to be used. For example, a thin Pt wire can be used in place of the Pt foil. The mass of the solder bath can be chosen so that the solder is always far from saturation even when the entire Pt wire has been consumed.

The activation energy observed in this study (16 kJ/mol based on linear kinetics) was considerably smaller than that reported in the literature. A value of 85.4 kJ/mol was reported for Pt dissolution into 40Pb-60Sn between 485°C and 535°C.[2] In this study,[2] a thin Pt wire was dissolved into a very large amount of solder so that the solder was always far from saturation. Linear dissolution kinetics was reported. Another value of 0.63 eV (or 60 kJ/mol) was reported for Pt dissolution into 40Pb-60Sn between 200°C and 320°C.[3] In this study,[3] a thin 40Pb-60Sn layer (100 μm) was used over Pt. The amount of solder used was small, and the solder was saturated with Pt rather quickly. Parabolic dissolution kinetics was observed. These two literature results reported two very different phenomena (linear versus parabolic kinetics; large versus small solder volume). Activation energies determined from different (linear/parabolic) kinetics should not be compared. From the above discussion, one knows that the way in which the experiments are carried out is important. In all previous studies, the Pt was evaluated alone. In the present study, Pt was evaluated side by side with Ni and Co under the same experimental conditions, and we positively confirmed that in the dissolution kinetics Pt performed better than Ni and Co under the same experimental conditions.

This study shows that the wetting of eutectic Pb-Sn solder on Pt was not as good as that on a Ni substrate when the RMA-type and water-soluble fluxes were used. As had been pointed out in the literature,[23,24] wetting characteristics are not only affected by the substrates but also by the types of fluxes applied. Using different fluxes is in fact equivalent to using different substrates because the solid/flux and liquid/flux interfacial tensions vary with flux type.[23,24] In short, to achieve good wetting, the type of flux used is no less important than the substrate itself. Consequently, if a new flux can be developed specifically for Pt substrates, there is hope that wetting characteristics better than those reported in this study can be achieved for Pt.

SUMMARY

The Pt dissolution rate into molten Sn at 250°C to 310°C was smaller than that of Ni. In fact, the Pt dissolution rates were less than one-half of the value for Ni at all investigated temperatures. From the wetting balance study, the wetting time of Pt was not quite as good as that of Ni. Nevertheless, the wetting characteristics of Pt were still acceptable for UBM and surface finish applications. In summary, as far as consumption rate and wetting characteristics are concerned, a single Pt layer does have the potential to serve as both the oxidation-protection layer and the diffusion barrier layer. Future studies should focus on joint strength evaluation and reliability verification.

During the reaction between Pt and molten Sn, the major reaction product was $PtSn_4$, although two other compounds, likely to be Pt_3Sn and Pt_2Sn_3, did form at higher temperature reactions (≥270°C). The dissolution followed linear kinetics, with an apparent activation energy of 16 kJ/mol.

ACKNOWLEDGEMENT

The financial support of the National Science Council of Taiwan through Grant NSC-95-2221-E-002-443-MY3 is acknowledged.

REFERENCES

1. W.G. Bader, *Weld. J.* 48, 551 (1969).
2. B. Meagher, D. Schwarcz, and M. Ohring, *J. Mater. Sci.* 31, 5479 (1996). doi:10.1007/BF01159320.
3. J.F. Kuhmann, C.H. Chiang, P. Harde, F. Reier, W. Oesterle, I. Urban, and A. Klein, *Mater. Sci. Eng. A* 242, 22 (1998). doi:10.1016/S0921-5093(97)00536-4.

4. B. Wiens, *Z. Metallk.* 91, 863 (2000).
5. M. Klein, B. Wiens, M. Hutter, H. Oppermann, R. Aschenbrenner, and H. Reichl, *Proc. 50th Electronic Components and Technology Conf.* (2000), pp. 40–45.
6. T.H. Kim and Y.H. Kim, *JOM* 56, 45 (2004). doi:10.1007/s11837-004-0111-9.
7. S.J. Wang and C.Y. Liu, *Acta Mater.* 55, 3327 (2007). doi:10.1016/j.actamat.2007.01.031.
8. S. Bader, W. Gust, and H. Hieber, *Acta Mater.* 43, 329 (1995).
9. D. Gur and M. Bamberger, *Acta Mater.* 46, 4917 (1998). doi:10.1016/S1359-6454(98)00192-X.
10. H.K. Kim, H.K. Liou, and K.N. Tu, *Appl. Phys. Lett.* 66, 2337 (1995). doi:10.1063/1.113975.
11. S.K. Kang, *Scr. Metall.* 14, 421 (1980). doi:10.1016/0036-9748(80)90338-5.
12. C.M. Liu (Master's thesis, National Central University, Taiwan, 2000).
13. W.J. Zhu, J. Wang, H.S. Liu, Z.P. Jin, and W.P. Gong, *Mater. Sci. Eng. A* 456, 109 (2007). doi:10.1016/j.msea.2006.11.117.
14. C.E. Ho, Y.M. Chen, and C.R. Kao, *J. Electron. Mater.* 28, 1231 (1999). doi:10.1007/s11664-999-0162-3.
15. C.E. Ho, R. Zheng, G.L. Luo, A.H. Lin, and C.R. Kao, *J. Electron. Mater.* 29, 1175 (2000). doi:10.1007/s11664-000-0010-y.
16. C.E. Ho, S.Y. Tsai, and C.R. Kao, *IEEE Trans. Adv. Packag.* 24, 493 (2001). doi:10.1109/6040.982835.
17. C.W. Chang, C.E. Ho, S.C. Yang, and C.R. Kao, *J. Electron. Mater.* 35, 1948 (2006). doi:10.1007/s11664-006-0298-3.
18. C.W. Chang, Q.P. Lee, C.E. Ho, and C.R. Kao, *J. Electron. Mater.* 35, 366 (2006). doi:10.1007/BF02692458.
19. J.Y. Tsai, C.W. Chang, C.E. Ho, Y.L. Lin, and C.R. Kao, *J. Electron. Mater.* 35, 65 (2006). doi:10.1007/s11664-006-0185-y.
20. J.Y. Tsai, C.W. Chang, Y.C. Shieh, Y.C. Hu, and C.R. Kao, *J. Electron. Mater.* 34, 182 (2005). doi:10.1007/s11664-005-0231-1.
21. Y. Wang and K.N. Tu, *Appl. Phys. Lett.* 67, 1069 (1995). doi:10.1063/1.114467.
22. H. Baker, *ASM Handbook, Vol. 3, Alloy Phase Diagrams* (Metals Park, OH: ASM Intl., 1992), p. 2.347.
23. J.I. Lee, S.W. Chen, H.Y. Chang, and C.M. Chen, *J. Electron. Mater.* 32, 117 (2003). doi:10.1007/s11664-003-0181-4.
24. H.Y. Chang, S.W. Chen, D.S.H. Wong, and H.F. Hsu, *J. Mater. Res.* 18, 1420 (2003). doi:10.1557/JMR.2003.0195.